Adsorption of hydrogen on the interface of a graphene/boron nitride hybrid atomic membrane

Ting Cao (曹霆),[1,2] Ji Feng (冯济),[1,*] and E. G. Wang (王恩哥)[1]
[1]*International Center for Quantum Materials, School of Physics, Peking University, Beijing, China*
[2]*Yuanpei College, Peking University, Beijing, China*
(Received 22 May 2011; revised manuscript received 18 July 2011; published 21 November 2011)

The synthesis of a graphene/boron nitride hybrid atomic membrane offers a novel class of line interface that is chemically coherent at the atomic scale. We employ first-principles calculations to study the adsorption of atomic hydrogen at the interface of the graphene/boron nitride monolayer. We demonstrate that hydrogen shows a remarkable selective affinity toward the zigzag-type interface in the hybrid material, with notably higher binding energy compared to the bulk graphene, boron nitride, or the armchair interface. We also show that hydrogen adsorption can be a potential route for tuning the electronic property of the hybrid atomic membrane. Our calculation indicates that adding hydrogen to the zigzag interface can cause a semiconductor-to-metal transition in the material.

DOI: 10.1103/PhysRevB.84.205447 PACS number(s): 68.43.Bc, 73.22.Pr, 61.48.Gh

I. INTRODUCTION

Atomically thin membranes, e.g., graphene and monolayer hexagonal boron nitride (BN), are attractive, low-dimension electronic materials.[1,2] Recently, graphene/BN hybrid atomic membranes have attracted a lot of interest.[3–7] The electronic and chemical dispositions of these hybrid atomic membranes differ either from graphene or from a BN monolayer. In accordance with previous calculations, the hybrid structure prefers phase segregation and forms kinetically stable domain structures.[4,8,9] This novel material is interesting in two important aspects. First, if the stoichiometry of graphene is much smaller than that of BN, then the hybrid is a model two-dimensional system in which a semimetallic phase (graphene) is embedded in a wide-gap semiconducting matrix (BN). If the stoichiometry of graphene is much larger than that of BN, the opposite case would happen. Second, the domainlike structure is bounded by an unusual class of line interfaces, which have well-defined local coordination and orientation protected by stable covalent bonding. This class of line interfaces ensures faithful inheritance of crystallographic orientation across them, making them dramatically different from usual grain boundaries.

Hydrogenation of graphene, realized experimentally with hydrogen plasma, has shown its potential for hydrogen storage and band gap engineering.[10–13] Unlike the physisorption of most molecules,[14,15] when a hydrogen atom is chemisorbed on graphene, it binds covalently to a carbon atom and changes its hybridization from planer sp^2 to sp^3. As the electronic structure near the Fermi level mainly originates from the covalent binding between the p_z orbital of each carbon atom, the hydrogen adatom passivates the local p_z orbital and therefore modifies the properties of graphene significantly.[16–20]

First-principles calculations have demonstrated that the electronic characteristics originating from the atomic p_z orbitals of the two-dimensional hybrid material largely depend on the interfacial structure.[6,7,21,22] Consequently, chemical modifications to the interfacial structure are a viable means to tune its properties with minimal perturbation to the underlying honeycomb lattice. Hydrogen adsorption, which is capable of altering the properties of pristine graphene sheets and nanoribbons considerably, will likely be a pathway toward tuning the properties of the hybrid structure. In graphene's case, although a lot of models based on patterned hydrogen adsorption have been proposed to suggest various attractive electronic and magnetic features,[23–26] these features rely sensitively on the distribution of adatoms. They are difficult to observe in experiments, since it is difficult to control the doses and positions of adatoms on an atomic scale. Therefore, it is important to investigate H adsorption on the hybrid structure. Previous research has indicated high chemical reactivity along the graphene nanoribbon's edge.[27] It is a natural question to ask whether this high reactivity toward chemical adsorption is preserved on the interface of BN and graphene. In this paper, we investigated atomic hydrogen adsorption on a single layer of hybridized BN and graphene. Both monomer adsorption and dimer adsorption are considered in our calculations.

II. METHODS

First-principles calculations were performed using spin-polarized density functional theory implemented in the Vienna *ab initio* simulation package[28,29] within the static lattice approximation. The projector-augmented wave method[30] was used with a Perdew-Burke-Ernzerhof functional[31] in the scheme of a generalized gradient approximation (GGA). The plane-wave energy cutoff was set to 500 eV, at which the variation of adsorption energy converges to within 10 meV. All atomic coordinates were optimized using a conjugated-gradient algorithm, with the forces on every atom converged to within 0.03 eV/Å. The size of supercell considered was carefully tested, and a vacuum layer of 15 Å was adopted to minimize interaction between periodic images. The supercells used are schematically displayed in Figs. 1(a) and 2(a). The number of **k**-points used to sample the Brillouin zone was 50, and the linear tetrahedron method with Blöchl corrections was used in the total energy calculation. The variation of adsorption energy in a supercell was within 3 meV if the number of **k**-points was increased to 100.

III. RESULTS

A. Structure

As a calibration, we first investigate the adsorption of a single hydrogen atom on pristine graphene and a BN

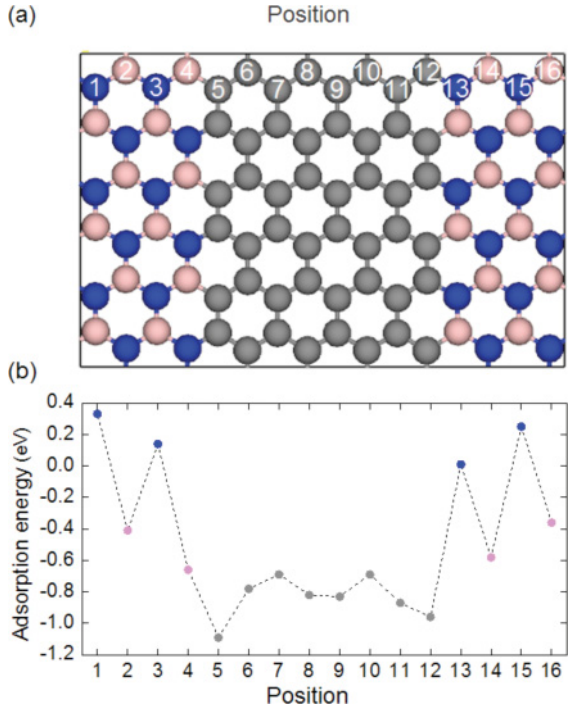

FIG. 1. (Color online) Adsorption energy of a single hydrogen atom on the armchair interface. (a) A schematic of the supercell. Pink (light gray), gray, and blue (dark gray) balls denote boron, carbon, and nitrogen atoms, respectively. White numbers marked on atoms denote different adsorption positions. (b) Adsorption energy of a hydrogen atom at different positions. The dotted line is a visual guide.

monolayer. The adsorption energy is defined as

$$E_{\text{ads}} = (E_{\text{X}+n\text{H}} - nE_{\text{H}} - E_{\text{X}})/n. \quad (1)$$

Here, the subscript X stands for the structure prior to hydrogen adsorption, as defined by the supercell used in calculations, and n stands for the number of adsorbed hydrogen atoms in a supercell. E_{ads} denotes the adsorption energy per hydrogen atom, $E_{\text{X}+n\text{H}}$ denotes the total energy of the adsorbed system, E_{H} denotes the energy of a single hydrogen atom, and E_{X} denotes the energy of the graphene/BN hybrid prior to adsorption of H.

When a hydrogen atom adsorbs on graphene, the most energetically favorable adsorption site is computed to be directly atop a carbon atom, as expected. The adsorption energy of -0.82 eV is substantially smaller than the average C-H bond strength of 4.3 eV in CH_4, in part because of the energy penalty coming from the strain induced in the graphene sheet by converting one C from planar sp^2 to tetrahedral sp^3 hybridization. When a hydrogen atom adsorbs on a BN monolayer, it binds either to a boron or to a nitrogen atom to form sp^3 hybridization. The adsorption binding energies are $+0.01$ or $+0.79$ eV (metastable), respectively. These results are consistent with previous first-principles calculations.[16–18,32]

As discussed in Sec. I, thermodynamically the most stable structure of the graphene/BN hybrid material features phase segregation.[4,8] Typically, the graphene/BN hybrid structure is synthesized in nonequilibrium processes, which can lead to rather irregular shapes of the interfaces. Here, we study the adsorptive property of this material and its impact on the transport properties. Therefore, we limit ourselves to the

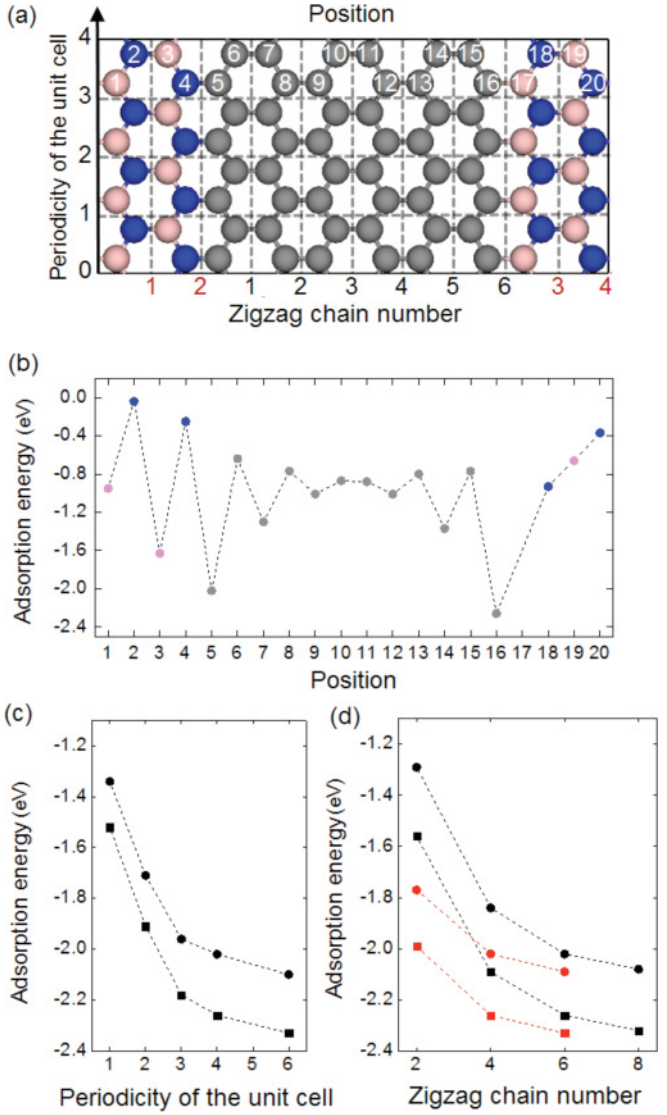

FIG. 2. (Color online) Adsorption energy of a single hydrogen atom on the zigzag interface. Dashed and dotted lines are visual guides. (a) A schematic of the supercell. Pink (light gray), gray, and blue (dark gray) balls denote boron, carbon, and nitrogen atoms, respectively. Red (gray) and black numbers at the bottom of the graph denote the zigzag chain number of BN and graphene, which measures the width of the BN and graphene stripe. White numbers marked on atoms denote different adsorption positions. (b) Adsorption energy of a hydrogen atom at different positions. (No stable structure was obtained for adsorption on position 17 during our structural optimization.) (c) Adsorption energy as a function of the periodicity of the unit cell. Circles and squares denote adsorption at carbon atoms next to nitrogen atoms and boron atoms, respectively. The zigzag chain number is fixed at 6 for graphene and 4 for BN. (d) Adsorption energy as a function of the zigzag chain number of the graphene (black) and BN (red [gray]) stripe. When the zigzag chain number of graphene or BN is changed, the corresponding number of BN or graphene is fixed at 4 or 6. Circles and squares denote adsorption at carbon atoms next to nitrogen atoms and boron atoms, respectively. The periodicity of the unit cell is fixed at 4.

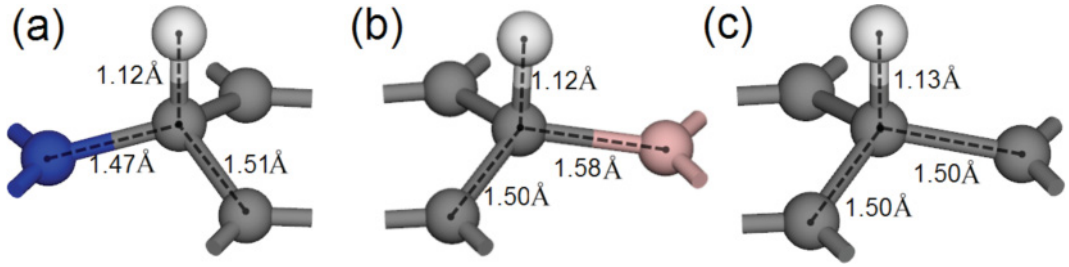

FIG. 3. (Color online) Local structures for single hydrogen atom adsorption on a carbon atom near (a) nitrogen and (b) boron. (c) Structure for single hydrogen atom adsorption on pristine graphene. White, pink (light gray), gray, and blue (dark gray) balls denote hydrogen, boron, carbon, and nitrogen atoms, respectively.

simplest models involving the only two chemically coherently linear boundaries (i.e., zigzag and armchair) to investigate the general feature of such interfaces upon hydrogen adsorption. Without topological defects (e.g., 5–7 rings), the graphene/BN interface should in principle be a combination of the two elementary types.

The two model systems adopted are shown in Figs. 1(a) and 2(a). In Fig. 1, we consider the armchair graphene nanoribbon embedded in a BN matrix. The bond lengths in these two systems prior to adsorption show a characteristic order, that is, C-N < C-C < C-B. The presence of the armchair interface leads to enhanced adsorption of hydrogen on carbon atoms compared to adsorption of a pristine graphene monolayer [Fig. 1(b)]. The largest binding affinity appears as the hydrogen atom binds to a carbon atom next to boron, with an adsorption energy of −1.09 eV.

The situation on the zigzag interface is quite different. In Fig. 2, we consider the zigzag graphene nanoribbon embedded in the BN matrix. The periodicity of the unit cell measures the separation between hydrogen adatoms in neighboring periodic images in the zigzag direction. The zigzag chain number measures the width of the graphene or BN stripe. As a topological property of the honeycomb lattice, the atoms at opposite zigzag edges belong to different sublattices. Consequently, the zigzag structure of hybrid graphene/BN presents a symmetry-broken chemical coordination compared to the pristine zigzag graphene nanoribbon, when a graphene nanoribbon is embedded in BN matrix. One interface of the zigzag structure connects carbon atoms and nitrogen atoms, whereas the other interface connects carbon atoms and boron atoms. The magnitude of the adsorption energy of a single hydrogen atom on the zigzag interface is significantly enhanced compared to the magnitude at other positions [Fig. 2(b)], as well as to that of pristine graphene. When the periodicity of the unit cell is 4, the zigzag chain number of graphene is 6, and that of BN is 4, then the adsorption energy can be as large as −2.26 eV, occurring at position 16. In the same structure, the second-strongest adsorption energy is at position 5, with $E_{\text{ads}} = -2.02$ eV, also on a carbon atom along the zigzag interface. Further enlargement of the model size (i.e., the periodicity of the unit cell, the zigzag chain number of graphene, and that of the BN stripe) only results in small changes in the adsorption energies [Fig. 2(c) and 2(d)]. Thus, our results represent quite well H adsorption in the dilute limit. This large enhancement of the adsorption energy from the zigzag interfaces to the bulk graphene can lead to the selective enrichment of H adatoms on the zigzag interface, identifiable experimentally by scanning tunneling microscopy imaging. This remarkable enhancement of adsorption affinity at the interface owes its origin to the electronic structure of the system, as will be discussed shortly.

The local structures of a hydrogen atom adsorbed on the zigzag interface and pristine graphene are displayed in Fig. 3. The carbon atom binding to hydrogen is lifted out of the plane by ∼0.51 and 0.38 Å when the carbon atom belongs to the C-N and C-B zigzag interface, respectively. This is to be compared to 0.48 Å in H adsorption on a pristine graphene monolayer, computed by the same method. Charge density analysis reveals that the variations of the total charge density inside the covalent radius of hydrogen atoms are all less than 0.05 electron in the preceding three cases. These results clearly show the characteristics of sp^3 geometry for the carbon atom that binds a H atom, regardless of where the hydrogen atom adsorbs.

We move on to the possibility of hydrogen dimer adsorption on the zigzag interface. It has been suggested that dimer adsorption is energetically preferred to adsorption of a single atom on pristine graphene.[16,17,19,33] The dimer configurations considered in this study were chosen according to previous research. The adsorption energy and the corresponding structure are shown in Fig. 4, with the calculations shown in Table I. The results indicate that as the first hydrogen atom binds preferentially to the carbon atom at the zigzag interface, further adsorption into dimer configurations leads to a decrease in the incremental adsorption energy and is accordingly less favorable than the adsorption of the first hydrogen atom. In addition, the largest adsorption energy per atom for hydrogen dimer on a bulk graphene is −1.37 eV, which is also considerably smaller than that on the zigzag interface of graphene and BN. Therefore, when the dose of the hydrogen atom is small and the whole system reaches the equilibrium state upon annealing, our calculations indicate that hydrogen atoms are primarily localized on the zigzag interface, dominated by a monomer configuration.

B. Electronic structure

Because the zigzag interface is relatively more prone to H adsorption, we discuss the influence of a single adatom on the electronic characteristics of the zigzag system. Several structures with different zigzag chain numbers and unit cell periodicities have been systematically tested. Our calculation

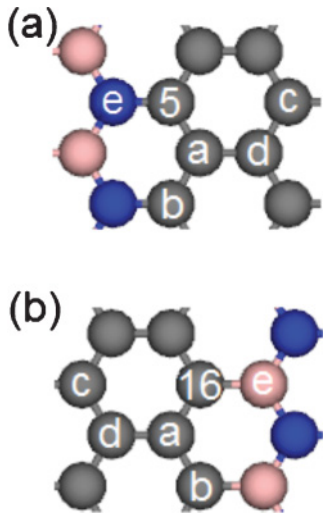

FIG. 4. (Color online) Local schematic of dimer adsorption configurations at the zigzag (a) C-N and (b) C-B interface. Numbers and letters denote the first and the second adsorption sites. Pink (light gray), gray, and blue (dark gray) balls denote boron, carbon, and nitrogen atoms, respectively.

shows a finite band gap exists before adsorption [Fig. 5(a)], which is consistent with the results obtained by others.[6] Spin-polarized and non–spin-polarized calculations were both employed, but the differences in the two energies (magnetic vs nonmagnetic) are always less than 30 meV per supercell, significantly smaller than the corresponding zero-point energy. This small energy difference indicates that there are likely two nearly degenerate ground states within the GGA scheme.

Despite the complications in magnetic properties, the metallic band structure appears upon hydrogen adsorption, as long as the zigzag chain number of graphene is larger than 4, in both magnetic and nonmagnetic ground states. What leads to the metallicity is quite similar to the "doping" mechanism frequently used in semiconductor physics.

Before the formation of the graphene/BN zigzag interface, there are electronic states localized at the zigzag carbon, boron, and nitrogen edge. These are akin to the edge states of graphene ribbons.[34] Upon the formation of the graphene/BN interface, the edge states from the graphene side and the BN side are allowed to interact, forming bonding and antibonding

TABLE I. Adsorption energy of different configurations. The calculations were performed in the supercell shown in Fig. 2(a).

Configuration	Adsorption energy per H atom (eV)	Adsorption energy of the second H atom (eV)
5-a	−1.61	−1.20
5-b	−1.61	−1.19
5-c	−1.68	−1.34
5-d	−1.52	−1.02
5-e	−1.66	−1.30
16-a	−1.68	−1.09
16-b	−1.80	−1.33
16-c	−1.75	−1.23
16-d	−1.65	−1.03
16-e	−1.51	−0.75

combinations. This is schematically shown in Fig. 5(b). As we can see, the on-site energy of p_z state on N is lower than that on C. Upon interaction, the p_z state of the abutting edge state of graphene gets pushed up in energy. In contrast, the p_z state of B lies above that of C. Consequently, the p_z state of the corresponding edge on graphene gets pushed down in energy. It is this different perturbation from the N and B termination at the interfaces that causes a small but finite band gap in the embedded graphene nanoribbon [Fig. 5(a)].

In Fig. 5(c), we show the partial electronic charge densities, corresponding to the distribution in real space of electronic states above and below Fermi level (in a 0.5-eV window). From the partial charge density distribution, we note the following: The highest occupied state mainly originates from the edge state at the C-B interface, and the lowest unoccupied state mainly originates from the edge state at the C-N interface. It can be observed from the graph that the partial charge density shows a clear nodal plane (zero electron density) between interfacial carbon and nitrogen atoms for the lowest unoccupied state, consequently corresponding to an antibonding state between the graphene edge state and the BN edge state at the N termination. The absence of a nodal plane between interfacial carbon and boron atoms for the highest occupied state indicates that it is a bonding state between the graphene edge state and the BN edge state at the B termination. The partial density of states (PDOS) from the carbon p_z orbitals at the interface confirms our analysis [Fig. 5(d)]. The splitting between the bonding and the antibonding combinations is the main origin of the band gap in the system, which is computed to be ∼50 meV. Although small, the size of the gap is about twice the energy corresponding to room temperature, and the intrinsic semiconducting behavior can be probed at low temperatures.

The effect of hydrogen adsorption is quite dramatic. After adsorption of a single hydrogen atom on one interface, the whole system becomes metallic. The partial charge density graph reveals that the electronic states in the vicinity of mainly Fermi level mainly localize at the other interface (Fig. 6). The mechanism for adsorption-induced metallization is again related to the edge states. The originally coherent zigzag interface is destroyed by the intrusion of the adsorbed hydrogen atom at the edge. Therefore, the previously localized edge state at this interface spreads over a large energy interval by interacting with the p_z states of the rest of the honeycomb network. The spectrally more diffuse manifold of electronic states on the hydrogen-adsorbing interface alters the electron filling, inducing a shift in Fermi level. As a consequence, the Fermi level crosses the other unaffected edge state.

This mechanism of metallization is schematically shown in Fig. 7(a) and 7(c). The supercell used in this illustration is the same as the one displayed in Fig. 2(a). When a hydrogen atom adsorbs at position 5, the energy difference between the magnetic state and the nonmagnetic state is within 3 meV per supercell, so we only show the PDOS of the nonmagnetic state [Fig. 7(b)]. When adsorption occurs at position 16, the magnetic ground state is energetically more stable than the nonmagnetic state by 8 meV, so the PDOS of the magnetic state is shown [Fig. 7(d)]. The computed gap closure upon the H addition is valid in both magnetic and nonmagnetic ground

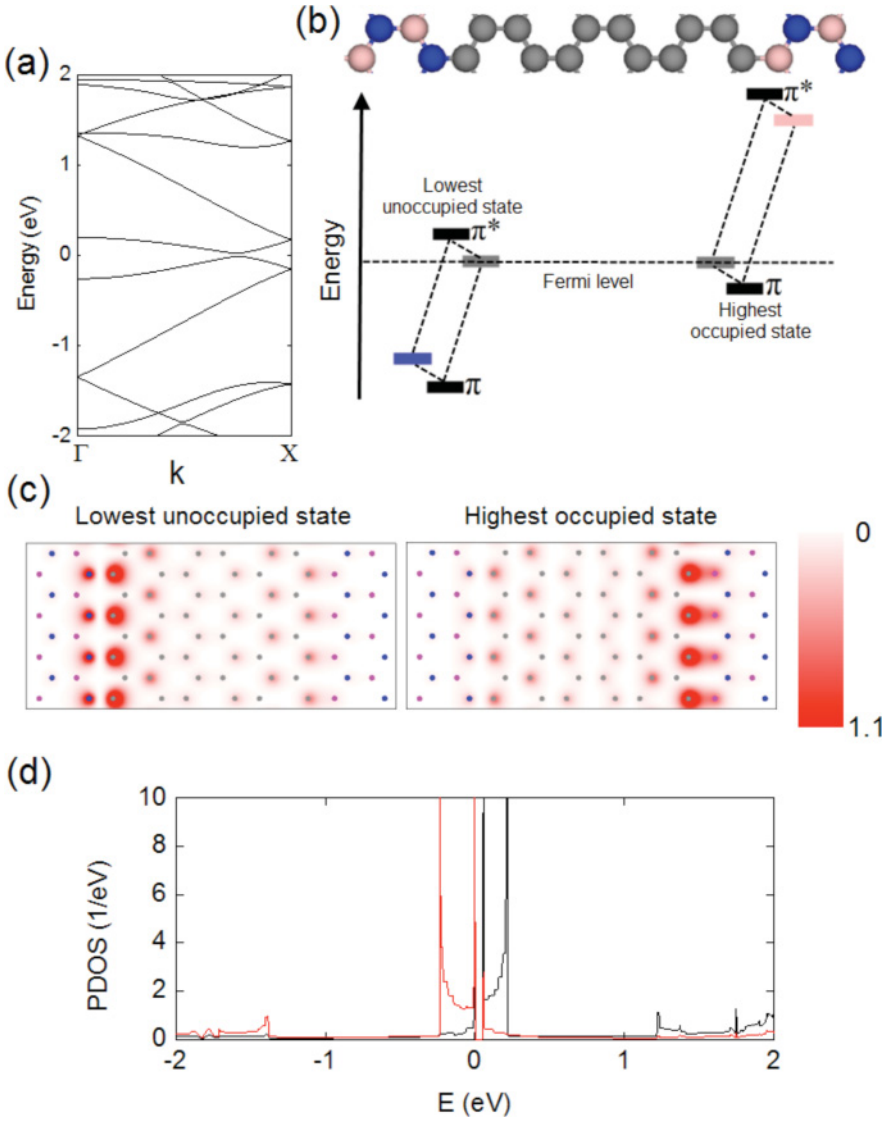

FIG. 5. (Color online) The electronic structure prior to adsorption. (a) The band structure prior to adsorption. (b) A schematic of the origin of the band gap. Pink (light gray), gray, and blue (dark gray) balls denote boron, carbon, and nitrogen atoms, respectively. The pink (light gray), gray, and blue (dark gray) bars denote electronic states localized at boron, carbon, and nitrogen edges, respectively, prior to the formation of graphene/BN interface. They hybridize to form bonding and antibonding edge states. (c) The partial charge density graph for lowest unoccupied and highest occupied states. The charge density is integrated in the direction perpendicular to the plane of graphene/BN hybrid structure. The energy intervals chosen for the highest occupied and the lowest unoccupied states are -0.5 to $+0$ eV (the Fermi level) and 0–0.5 eV, respectively. The scale bar is in units of -10^{-1} $|e|\text{Å}^{-2}$. Pink (light gray), gray, and blue (dark gray) dots denote boron, carbon, and nitrogen atoms, respectively. (d) The PDOS diagram from the carbon p_z orbitals at the C-B interface (red [gray]) and the C-N interface (black). The unit cell used is shown in Fig. 2(a).

states. In addition, when the periodicity of the supercell further increases, the band structure shows the half-metallic feature upon hydrogen adsorption. The half metallicity of the interface prior to hydrogen adsorption was noted in a calculation using a localized basis set,[6] where a possible explanation was also suggested.

The special binding affinity of the zigzag interface could also be unveiled in terms of the modulation of the edge state upon hydrogen adsorption. Concerning adsorption of a single hydrogen atom on the bulk graphene, the bonding of the π-conjugated system is broken, with ensuing formation of sp^3 hybridization. In contrast, at the zigzag interface, the

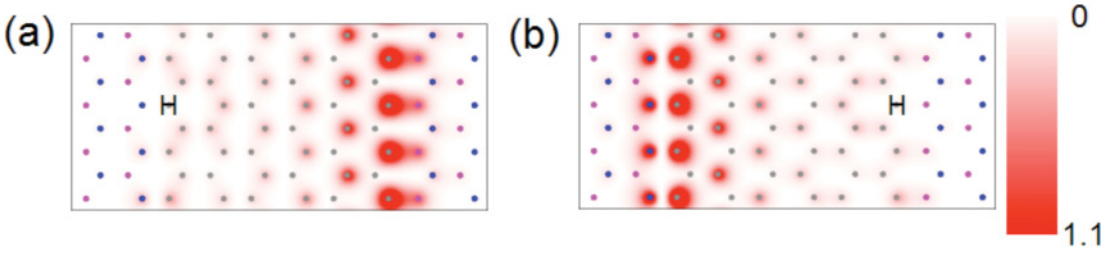

FIG. 6. (Color online) The partial charge density graph after adsorption of a single hydrogen atom on (a) position 5 and (b) position 16. Pink (light gray), gray, and blue (dark gray) dots denote boron, carbon, and nitrogen atoms, respectively. The energy interval is chosen to be -0.25 to $+0.25$ eV (relative to the Fermi level). The partial charge density is summed over spin-up and spin-down components in (b). Other conventions are followed from Fig. 5(c).

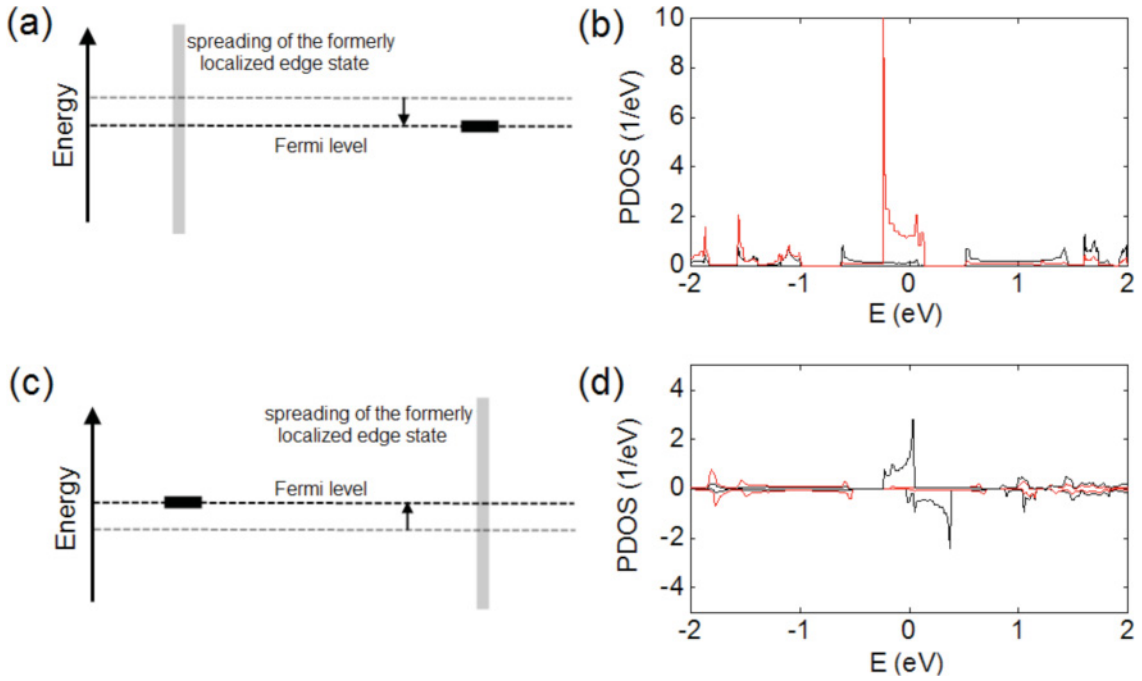

FIG. 7. (Color online) Origin of metallicity upon adsorption. (a) A schematic of the electronic structure after adsorption on position 5. (b) The PDOS diagram from the unpassivated carbon p_z orbitals at the C-B interface (red) and the C-N interface (black) after adsorption on position 5. (c) A schematic of the electronic structure after adsorption on position 16. (d) The PDOS diagram after adsorption on position 16. In this diagram, the plus and minus values indicate spin-up and spin-down components, respectively.

edge states derived from the p_z orbitals prior to adsorption mainly localize on the interfacial carbon atoms [Fig. 5(c)], displaying little energy dispersion compared to the bulk graphene [Fig. 5(d)]. Thus, in the zigzag interface, the bonding of the π electrons between the interfacial carbon atoms and those in the bulk is rather weak compared to the bonding of the bulk graphene. The energy cost to break the bonding between the π electrons is less at the zigzag interface than at the bulk graphene. Put somewhat differently, the energies of the edge states are within a narrow window around the Fermi level, while the energies of the graphene's occupied p_z states have a large dispersion over a ~8.4-eV window below the Fermi level. Therefore, it carries a larger energy penalty to extract one carbon atom from the bulk p_z states than from the edge. As a result, the magnitude of adsorption energy of a single hydrogen atom on a carbon atom at the zigzag interface is larger than the corresponding bulk value. When the second hydrogen atom adsorbs on the interfacial carbon atom next to the previously adsorbed one, the magnitude of its adsorption energy decreases significantly compared to that of the first one (5-b and 16-b in Fig. 4 and Table I). This is because the adsorption of the first hydrogen atom has eliminated the formerly localized edge state at this interface (Fig. 6). The arguments given here are general and thus applicable to interfacial structures with localized edge states, which should generally enhance adsorption that leads to one single-bond attachment (C-H bond in our case).

IV. CONCLUSIONS

Zigzag graphene nanoribbons have long been considered promising candidates for electronic engineering because of the existence of a finite band gap.[23,35] The successful synthesis of a BN and graphene heterostructure opens a new way to engineer the potential band gap at different types of interfaces. Our detailed first-principles calculations reveal a remarkable selective affinity toward the zigzag-type interface in the hybrid material by hydrogen adsorption, with notably higher binding energy compared to that of the bulk graphene, BN, or graphene/BN armchair interface. In addition, the adsorbed hydrogen atom induces a transition in the material from the semiconducting state to the metallic state. In experiments, controlled hydrogen adsorption on the zigzag interface can be initiated with hydrogen plasma by adjusting the reaction condition. In the subsequent annealing process, hydrogen atoms are expected, from our results, to migrate to the potential minimum and finally localize at the zigzag interface. The transition from a semiconducting to a metallic state upon adsorption of the hydrogen atom on the zigzag interface is potentially a pathway toward band gap engineering of this two-dimensional hybrid atomic membrane. Finally, the whole system is computed to possess a half-metallic property upon hydrogen adsorption in the dilute limit. Even though the energy difference is small between magnetic and nonmagnetic ground states, the possibility of spin-polarized transport property should not be ruled out.

ACKNOWLEDGMENTS

The work was supported by NSFC (Projects 10974238, 91021007 and 11174009) and MOST of China. T.C. thanks Q. Zhou, Z. Bi, X. B. Guo, D. L. Xie, and X. M. Liu for useful discussions.

*jfeng11@pku.edu.cn

[1] A. K. Geim and K. S. Novoselov, Nat. Mater. **6**, 183 (2007).

[2] C. Jin, F. Lin, K. Suenaga, and S. Iijima, Phys. Rev. Lett. **102**, 195505 (2009).

[3] L. Ci, L. Song, C. H. Jin, D. Jariwala, D. X. Wu, Y. J. Li, A. Srivastava, Z. F. Wang, K. Storr, L. Balicas, F. Liu, and P. M. Ajayan, Nat. Mater. **9**, 430 (2010).

[4] J. D. Martins and H. Chacham, ACS Nano **5**, 385 (2010).

[5] K. Raidongia, A. Nag, K. P. S. S. Hembram, U. V. Waghmare, R. Datta, and C. N. R. Rao, Chem. Eur. J. **16**, 149 (2010).

[6] J. M. Pruneda, Phys. Rev. B **81**, 161409 (2010).

[7] S. Dutta, A. K. Manna, and S. K. Pati, Phys. Rev. Lett. **102**, 096601 (2009).

[8] K. Yuge, Phys. Rev. B **79**, 144109 (2009).

[9] J. Zhu, S. Bhandary, B. Sanyal, and H. Ottosson, J. Phys. Chem. C **115**, 10264 (2011).

[10] R. Balog, B. Jorgensen, L. Nilsson, M. Andersen, E. Rienks, M. Bianchi, M. Fanetti, E. Laegsgaard, A. Baraldi, S. Lizzit, Z. Sljivancanin, F. Besenbacher, B. Hammer, T. G. Pedersen, P. Hofmann, and L. Hornekaer, Nat. Mater. **9**, 315 (2010).

[11] R. Balog, B. Jorgensen, J. Wells, E. Laegsgaard, P. Hofmann, F. Besenbacher, and L. Hornekaer, J. Am. Chem. Soc. **131**, 8744 (2009).

[12] D. C. Elias, R. R. Nair, T. M. G. Mohiuddin, S. V. Morozov, P. Blake, M. P. Halsall, A. C. Ferrari, D. W. Boukhvalov, M. I. Katsnelson, A. K. Geim, and K. S. Novoselov, Science **323**, 610 (2009).

[13] N. P. Guisinger, G. M. Rutter, J. N. Crain, P. N. First, and J. A. Stroscio, Nano Lett. **9**, 1462 (2009).

[14] T. O. Wehling, M. I. Katsnelson, and A. I. Lichtenstein, Phys. Rev. B **80**, 085428 (2009).

[15] O. Leenaerts, B. Partoens, and F. M. Peeters, Phys. Rev. B **77**, 125416 (2008).

[16] S. Casolo, O. M. Lovvik, R. Martinazzo, and G. F. Tantardini, J. Chem. Phys. **130**, 054704 (2009).

[17] L. Hornekær, Ž. Šljivančanin, W. Xu, R. Otero, E. Rauls, I. Stensgaard, E. Lægsgaard, B. Hammer, and F. Besenbacher, Phys. Rev. Lett. **96**, 156104 (2006).

[18] A. Ranjbar, M. S. Bahramy, M. Khazaei, H. Mizuseki, and Y. Kawazoe, Phys. Rev. B **82**, 165446 (2010).

[19] D. W. Boukhvalov, M. I. Katsnelson, and A. I. Lichtenstein, Phys. Rev. B **77**, 035427 (2008).

[20] J. Berashevich and T. Chakraborty, Phys. Rev. B **82**, 134415 (2010).

[21] Y. Ding, Y. Wang, and J. Ni, Appl. Phys. Lett. **95**, 123105 (2009).

[22] J. He, K.-Q. Chen, Z.-Q. Fan, L.-M. Tang, and W. P. Hu, Appl. Phys. Lett. **97**, 193305 (2010).

[23] H. J. Xiang, E. J. Kan, S. H. Wei, M. H. Whangbo, and J. L. Yang, Nano Lett. **9**, 4025 (2009).

[24] D. Soriano, F. Muñoz-Rojas, J. Fernández-Rossier, and J. J. Palacios, Phys. Rev. B **81**, 165409 (2010).

[25] M. J. Schmidt and D. Loss, Phys. Rev. B **82**, 085422 (2010).

[26] H. Şahin, C. Ataca, and S. Ciraci, Phys. Rev. B **81**, 205417 (2010).

[27] D.-E. Jiang, B. G. Sumpter, and S. Dai, J. Chem. Phys. **126**, 134701 (2007).

[28] G. Kresse and J. Hafner, Phys. Rev. B **49**, 14251 (1994).

[29] G. Kresse and J. Hafner, Phys. Rev. B **47**, 558 (1993).

[30] G. Kresse and D. Joubert, Phys. Rev. B **59**, 1758 (1999).

[31] J. P. Perdew, K. Burke, and M. Ernzerhof, Phys. Rev. Lett. **77**, 3865 (1996).

[32] P. F. Weck, E. Kim, S. H. Lepp, N. Balakrishnan, and H. R. Sadeghpour, Phys. Chem. Chem. Phys. **10**, 5184 (2008).

[33] Y. Ferro, D. Teillet-Billy, N. Rougeau, V. Sidis, S. Morisset, and A. Allouche, Phys. Rev. B **78**, 085417 (2008).

[34] K. Nakada, M. Fujita, G. Dresselhaus, and M. S. Dresselhaus, Phys. Rev. B **54**, 17954 (1996).

[35] Y.-W. Son, M. L. Cohen, and S. G. Louie, Nature (London) **444**, 347 (2006).